N90-28272

SEASONAL AND INTERANNUAL CHANGES IN CIRRUS

Donald Wylie
Space Science and Engineering Center
University of Wisconsin-Madison

1. Introduction

Statistics on cirrus clouds using the multispectral data from the GOES/VAS satellite have been collected since 1985. The method used to diagnose cirrus clouds and a summary of the first two years of data was given in Wylie and Menzel (1989) and at the 1988 FIRE Meeting in Vail, CO. This study has been expanded to three years of data which allows a more detailed discussion of the geographical and seasonal changes in cloud cover. Interannual changes in cloud cover also have been studied.

GOES/VAS cloud retrievals also have been compared to atmospheric dynamic parameters and to radiative attenuation data taken by a lidar. This abstract will discuss some of the highlights of these studies.

2. Geographical Distributions

Fig. 1 summarizes the geographical distribution of cloud cover over three year. This summary is very similar to the two year graphic in Wylie and Menzel (1989) except for some small regional features which appear because finer contour intervals were used (10% probability rather than the 20% previously used). This was possible because the increase in cloud observations from the extra year of data.

Similar winter to summer seasonal changes in the locations of cloud cover minima (top panels) and clear sky maxima (bottom panels) can be found in the three year summary as in the previously published summary. The same migration of the "sun belt" from Arizona and New Mexico in the winter (upper left panel) to southern California and southern Nevada in the summer (upper right) is apparent. The Probability of Clear Sky (lower panels) show the same general trends as the Probability of Opaque Cloud (upper panels) between the seasons.

Other seasonal changes include the increase of cloud cover off the California coast (top panel) as the marine stratus clouds become predominant in summer. A minimum in cloud cover along the East Coast appears in winter (upper left panel) and disappears in summer. A local maximum in opaque cloud cover occurred along the Appalachian mountains in the summer (upper right). Other cloud cover maxima were found in Washington and Oregon corresponding to the Coastal mountains.

Differences with the previous results can be found in western Missouri over part of the Ozark mountains in summer and over Lake Michigan in winter where small opaque cloud maxima are now apparent. The Northern Rocky mountains in Idaho and Montana show more local detail in both seasons. All of these features were in the previously published data but hidden by the choice of a large contour interval.

In the summer of 1988, an opaque cloud minima was found in central Montana extending down into Wyoming (upper right) which was part of the extreme drought.

Cirrus clouds (middle panels) exhibited very small geographical and seasonal variances over the continental U.S as previously published. They were found 20-40% of the time with a slight drop in the summer over the continent and a large drop over the Eastern Pacific ocean.

3. Interannual Variances

The variances in cloud cover between 1988 and 1987 were examined because the extreme drought and heat in the summer of 1988. The largest deficit in rainfall occurred in south and Ohio Valley in June, the states of Indiana, Ohio, Kentucky, Tennessee, Mississippi, Alabama, and Georgia according to Ropelewski (1988) see Fig. 2. Other rainfall deficiencies were found in the Midwest and northern plains states. The drought areas are indicated with shading in Fig. 2. But in June 1987, the drought areas received nearly normal precipitation (Arkin, 1988).

Cloud analyses from the two Junes were compared in the area of largest drought, form 30-42^{o}N and 82-90^{o}W (the box in Fig. 2). The GOES/VAS cloud analysis showed a decrease in high clouds, <400 mb, which was mainly cirrus (Table 1, 24% in June 87 compared to 20% in 88) and also a decrease in mid level clouds, 400-699 mb, (13% in 87 vs. 7% in 88). While low cloud reports increase from 24% in 87 to 33% in 88. The number of clear sky reports was nearly constant between the two years. These data indicate a change in the type of clouds found in this area between the two years. An large increase in low cloud occurred which were non-precipitating at the expense of deeper middle and high clouds.

Table 1: A comparison of GOES/VAS cloud analyses in the area, 30-42^{o} N, 82-90^{o}W, (box in Fig. 2) for June of 87 and 88.

		June 1987			June 1988		
Cloud Type		Cirrus	Opaque	All	Cirrus	Opaque	All
High	<400 mb	24%	4%	28%	20%	4%	24%
Middle	400-700mb	4	9	13	3	4	7
Low	>700 mb		24	24		33	33
Total		28%	37%	65%	23%	41%	64%
Clear				35%			36%

4. Comparison to Atmospheric Dynamic Features

Cirrus cloud observations from the GOES/VAS system were inspected to see what fraction were found inside dynamic features commonly thought to produce clouds and what fraction occurred outside of these dynamic features or in areas where dissipation of clouds was expected. This is an extension of the statistics presented at the 1988 FIRE meeting. More analyses have been added in more seasons.

The conclusions remain the same as last year. In summer, roughly one half of the cirrus observations were found near radar echoes while the other half was not. In winter this dropped to only 22% of the cirrus obs. being near radar echoes. No new data were added for this part of the comparison. Jet streams of >35 ms^{-1} in winter and >25 ms^{-1} in other seasons, contained 40 to 60% of the cirrus. However, in months when upper level winds were light, cirrus observations were found with nearly the same frequency as when winds were strong. Inside the jet stream most cirrus, 13 to 33%, were found accelerating into the entrance to the south of the jet axis (right rear quadrant). While the least cirrus were found, 4 to 10%, north of the axis in the entrance region (left rear quadrant). Approximately 20 to 23% of the cirrus were found in the exit of the jet core, the deceleration region (from left and right quadrants). Warm temperature advection was found with 44 to 71% of the cirrus in months where winds were high enough to define jet streams and temperature advection. Positive vorticity advection was found with 24 to 52% of the cirrus. However, a substantial amount of cirrus, from 19 to 35%, also occurred in negative vorticity advection.

These statistics show that large scale dynamics can explain up to one half of the cirrus over the U.S. Most of the other cirrus occurs in areas where the dynamic variables are weak or in a

transition from a positive to negative sign. The great complexity of the structure of cirrus and the thermodynamic conditions in which they were found is discussed in Starr and Wylie (1989). Greater detail in the analysis of atmospheric dynamic and thermodynamic features is needed to explain a large portion of the cirrus.

5. Comparison of Satellite with Lidar Radiative Properties

The GOES/VAS cloud analysis system estimates both the height of the cloud top and the emissivity of the cloud. This is defined as;

$$N\epsilon = \frac{I - I_{cl}}{B[T(P_c)] - I_{cl}}. \qquad (1)$$

I is the radiance of the cloud measured by the satellite in the 11.1μ window channel. I_{cl} is the clear radiance of the window channel estimated for the location from surrounding clear fields of view N and $B[T(P_c)]$ is the radiance for the altitude temperature of the cloud. $N\epsilon$ is thus an effective emmissivity that is the product of the clouds fractional coverage of the satellite field of view (N) and the emissivity (ϵ) of the cloud.

The infrared emissivity of cirrus clouds is related to the visible optical depth in that the lower the emittance of the cloud, the smaller its optical depth and reflectivity. There have been several models of this relationship. For this study the model of Hansen (1971) was used. Optical depths were measured by the HSRL lidar at UW on 28 October 1986. The mean altitude of the cirrus cloud was also taken from the lidar backscatter vertical profile while the infrared radiance of the cloud (I) and clear sky (I_{cl}) was measured by the GOES satellite. The radiance for the altitude of the cloud (B(T(p))), was derived from the mean cirrus cloud altitude and the temperature for that level given by a local sounding.

The results of the visible optical depth and infrared emissivity comparison are shown in Fig. 4. The model prediction of Hansen (1971) also is shown as a solid line. These data have a lot of scatter, however, they are distributed around the model results of Hansen. A comparison of similar visible and infrared data to model predictions is given in Minnis *et al.* (1989).

6. References

Arkin, P.A., 1988: The global climate for June-August 1987: Mature phase of an ENSO warm episode persists., *J. Climate*, **1**, 306-324.

Hansen, J.E., 1971: Multiple scattering of polarized light in planetary atmospheres. Part I: The doubling method., *J. Atmos. Sci.*, 120-125.

Minnis, P.A., D.F. Young, K. Sassen, J. M. Alvarez, and C. Grund, 1989: The 27-28 October 1986 FIRE IFO cirrus case study: Cirrus parameter relationships derived from satellite and lidar data., Submitted to *Mon. Wea. Rev.*

Ropelewski, C.F., 1988: The global climate for June-August 1988: A swing to the positive phase of the southern oscillation, drought in the United States, and abundant rain in monsoon areas., *J. Climate*, **1**, 1153-1174.

Wylie, D.P., and W.P. Menzel, 1989: Two years of cloud cover statistics using VAS., *J. Climate*, **2**, 380-392.

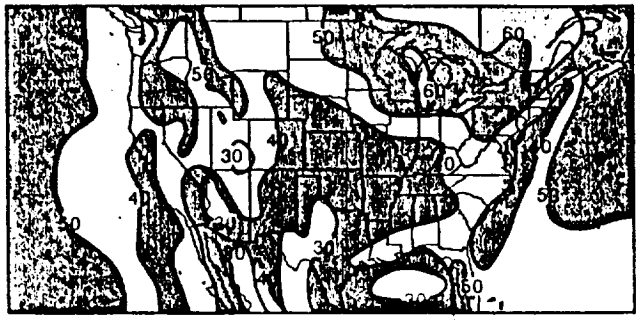

PROBABILITY OF OPAQUE CLOUD IN WINTER

PROBABILITY OF OPAQUE CLOUD IN SUMMER

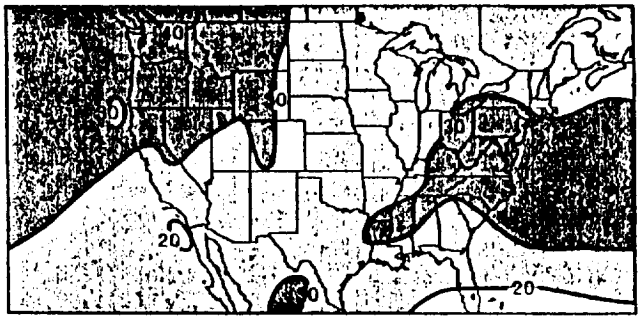

PROBABILITY OF CIRRUS IN WINTER

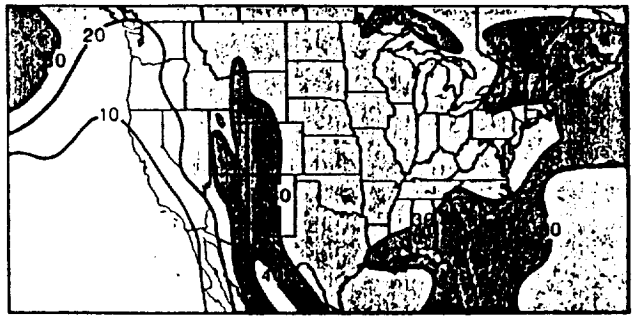

PROBABILITY OF CIRRUS IN SUMMER

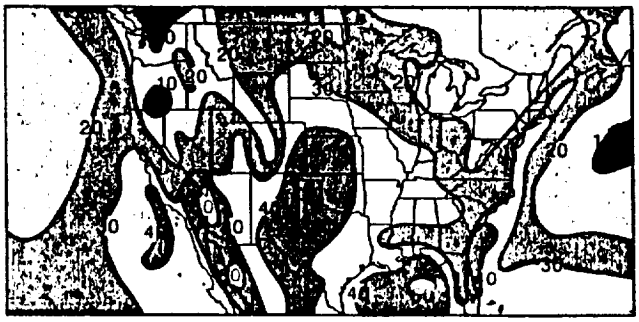

PROBABILITY OF CLEAR SKY IN WINTER

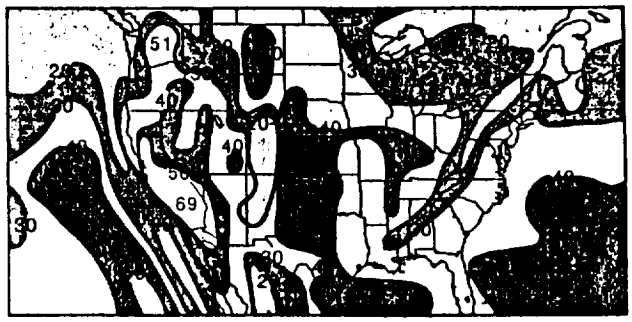

PROBABILITY OF CLEAR SKY IN SUMMER

THREE YEAR SUMMARY

WYLIE/MENZEL UNIV OF WISCONSIN-MADISON

Figure 1: The probability of opaque cloud, transmissive cirrus cloud, or clear sky from the GOES/VAS multispectral infrared data from 1985 to 1988.

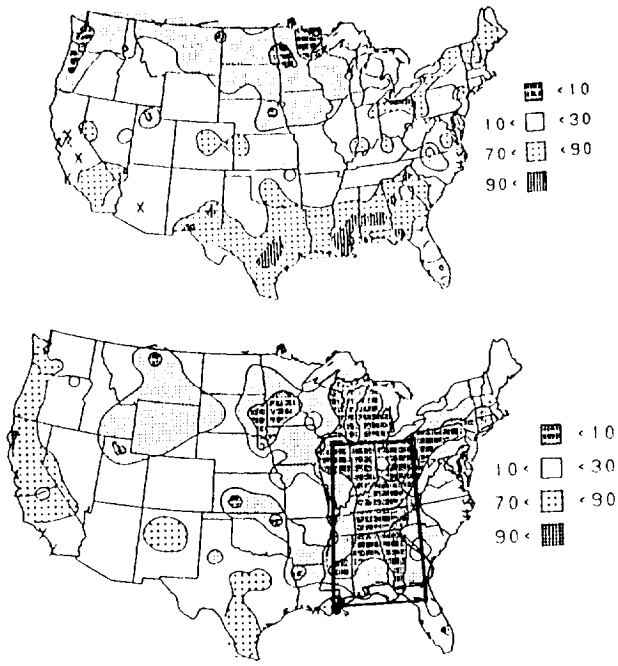

Figure 2: The June 1987 precipitation expressed as percentiles of the normal (Gausian) distribution from Arkin (1987), upper panel, and June 1988 from Ropelewski (1988), lower panel.

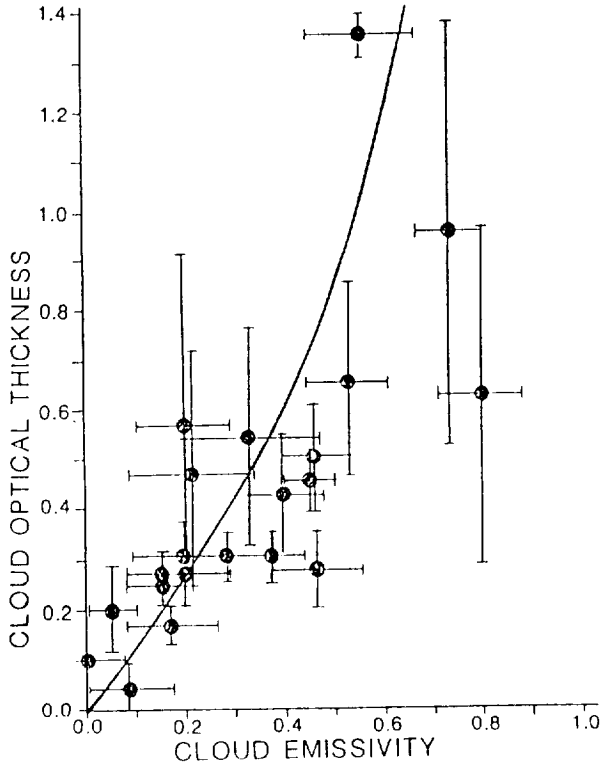

Figure 3: Cloud optical thickness measured by the HSRL lidar vs. Infrared emissivity measured from GOES/VAS satellite imagery.